Nat. Hazards Earth Syst. Sci. Discuss., doi:10.5194/nhess-2016-316, 2016
Manuscript under review for journal Nat. Hazards Earth Syst. Sci.
Published: 7 October 2016

Natural Hazards and Earth System Sciences
Discussions

Brief communication "3D reconstruction of a collapsed rock pillar from web-retrieved images and terrestrial LiDAR data – The 2005 event of the West face of the Drus (Mont-Blanc massif)"

Antoine Guerin[1], Antonio Abellán[2], Battista Matasci[3], Michel Jaboyedoff[1], Marc-Henri Derron[1] and Ludovic Ravanel[4]

[1]Risk Analysis Group, Institute of Earth Sciences, University of Lausanne, Switzerland
[2]Scott Polar Research Institute, University of Cambridge, United Kingdom
[3]Bureau d'Etudes Géologiques SA, Aproz, Switzerland
[4]EDYTEM, University Savoie Mont Blanc – CNRS, Le Bourget du Lac, France

Correspondence to: Antoine Guerin (antoine.guerin@unil.ch)

Abstract. In June 2005, a series of major rockfall events completely wiped out the Bonatti Pillar located in the legendary Drus West face (Mont-Blanc massif, France). Terrestrial LiDAR scans of the face were acquired after this event but no pre-event point cloud is available. Thus, in order to reconstruct the volume and the shape of the collapsed blocks, a 3D model has been built using photogrammetry (SfM) based on 30 pictures collected on the Web. All these pictures were taken between September 2003 and May 2005. We then reconstructed the shape and volume of the fallen compartment by comparing the SfM model with terrestrial LiDAR data acquired in October 2005 and November 2011. The volume is calculated to 292'680 m^3 (± 5 %). This result is close to the value previously assessed by Ravanel and Deline (2008) for this same rock-avalanche (265'000 ± 10'000 m^3). The difference between these two estimations can be explained by the rounded shape of the volume determined by photogrammetry, which may lead to a volume overestimation. However it is not excluded that the volume calculated by Ravanel and Deline (2008) is slightly underestimated, the thickness of the blocks having been assessed manually from historical photographs.

1 Introduction

The Drus (3'754 m a.s.l.) are emblematic summits of the Chamonix valley situated in the Mont-Blanc Massif (France). Since the middle of last century, the Petit Dru West face (1000 m-high, 3'730 m a.s.l.) is affected by intense erosion which has significantly modified the morphology of this peak (Ravanel and Deline, 2006 and 2008; Fort et al., 2009). In June 2005, a rock pillar (the Bonatti Pillar) estimated to be around 265'000 ± 10'000 m^3 by Ravanel and Deline (2008) collapsed, destroying forever numerous legendary climbing routes. The assessment of this volume by Ravanel and Deline (2008) was performed in two steps: (a) determination of the rock-avalanche scar dimensions (height and width) by making measurements on terrestrial LiDAR data acquired just after the event (October 2005); and (b) estimation of the thickness of the fallen blocks from historical photographs taken from different viewpoints. Note that these LiDAR scans correspond to

Nat. Hazards Earth Syst. Sci. Discuss., doi:10.5194/nhess-2016-316, 2016
Manuscript under review for journal Nat. Hazards Earth Syst. Sci.
Published: 7 October 2016

Natural Hazards and Earth System Sciences Discussions

the oldest reference and no 3D model is available before the major event of June 2005. Thus, in order to get the pre-event topography of the Petit Dru, we collected several pictures dating from 2003 to 2005 from different web picture hosting services and a 3D photogrammetric model was reconstructed. Such an approach was already used in different research areas such as cultural heritage conservation: precursor of this "crowdsourced" technics, Grün et al. (2004 and 2005) reproduced in 3D the statue of the Great Buddha of Bamiyan (Afghanistan) using a series of pictures obtained from the Internet. More recently, many historians, archaeologists or architects (e.g. Furukawa et al., 2010; Doulamis et al., 2013; Ioannides et al., 2013; Kyriakaki et al., 2014; Santos et al., 2014) took advantage of the large amount of images available online to preserve and keep a digital record of cultural and historical heritage using Structure-from-Motion (SfM) algorithms (Snavely et al., 2008). According to the *New York Times* (Estrin J., 2012), over 380 million pictures are uploaded on Facebook every day and other authors such as Stathopoulou et al. (2015) or Vincent et al. (2015) have used crowdsourced imagery to virtually replicate heritage objects destroyed by natural disasters, armed conflict or terrorism. Examples include the stone bridge of Plaka (Greece), the Kathmandu city before and after the 2015 Earthquake and several artworks at the Mosul Museum (Iraq).

In geosciences, conventional photogrammetry has long been used for Digital Elevation Model (DEM) generation but it is only recently that SfM has popularized the use of 3D point clouds in this field (e.g. Firpo et al., 2011; Salvini et al., 2013; James and Robson, 2014; Lucieer et al., 2014). This method is surprisingly straightforward to implement and also relatively accurate when compared with Terrestrial Laser Scanning (TLS) data. In 2013, Fonstad et al. obtained differences of about 0.1 m (in X, Y and Z) between these two methods. In addition, new technologies such as Unmanned Aerial Vehicles (UAV) combined with SfM have modernized investigations on several Earth surface phenomena (Abellán et al., 2016). For instance, Turner et al. (2012) and Lucieer et al. (2014) obtained 4 cm errors comparing DEM from UAV-SfM to Differential Global Positioning System (DGPS) ground control points. However, despite all these recent advances, paleotopographic reconstruction based on old images or orthophotos has been rarely used in the field of geohazards to improve erosion rate quantification (Oikonomidis et al., 2016). For this reason, the aim of this Short Note is to illustrate the potential to merge ground-based LiDAR measurements with SfM point clouds made from publicly available images. This allows traveling back in time in order to better quantify past natural disasters. More specifically, this Short Note reports the results of the 3D reconstruction of the Drus West face before the Bonatti Pillar collapse in June 2005.

1.1 Geological and structural setting

From a geological point of view, the Mont-Blanc crystalline range describes a broad ellipse elongated in the NE-SW direction extending from the Val Ferret (Valais, Switzerland) to the Chapieux Valley (Savoie, France) (Fig. 1A). The central part of the massif develops on the Aosta Valley (Italy) and Haute-Savoie (France) and it consists of two major petrological units: plutonic rocks (granites), mainly, and metamorphic rocks (gneiss and micaschists) which merge near the summit of Mont-Blanc (Fig. 1B). From Southwest to Northeast, granites also pass of an intrusive position in gneiss to a tectonic contact materialized by the Angle fault (Leloup et al., 2005). The Petit Dru West face presents a coarse-grained calk-alkaline granite,

Nat. Hazards Earth Syst. Sci. Discuss., doi:10.5194/nhess-2016-316, 2016
Manuscript under review for journal Nat. Hazards Earth Syst. Sci.
Published: 7 October 2016

Natural Hazards and Earth System Sciences Discussions

which was formed during the Hercynian orogeny and dated from 305 ± 2 million years (Bussy et al., 1989; von Raumer and Bussy, 2004; Egli and Mancktelow, 2013). The steep rock cliff (average dip of 75°) is cut by a set of two large sub-vertical fractures oriented 238°/85° and 303°/79° which form wedges and by four other joint sets (especially 106°/33°) which form deep overhangs (Ravanel and Deline, 2008; Matasci et al., 2015). These very persistent dihedral structures (mean trace length of 80 m) promote the collapse of large compartments and have played a major role (Matasci et al., 2015) during the large rockfall events of summer 2005 and fall 2011 (Fig. 1C).

<< FIGURE 1 >>

2 Material and methods

The 3D reconstruction of the Drus West face was carried out using 30 web-retrieved images from different picture hosting services (*Flickr.com*, *SummitPost.org* and *Camptocamp.org*, see Appendix A) and a commercial photogrammetric software (Agisoft PhotoScan – version 1.0.3). An estimation of the missing volume was then performed on 3DReshaper (2014 MR1 version) software by comparing the SfM point cloud with terrestrial LiDAR scans acquired after the event.

2.1 Selection of photographs from Internet

Before the June 2005 rock-avalanche, the Drus West face was affected by major rockfalls in September 1997 (27'500 ± 2'500 m^3) and August 2003 (6'500 ± 500 m^3) (Ravanel and Deline, 2008). These events have significantly modified the morphology of the pillar between 3'160 m a.s.l. and 3'460 m a.s.l. (Fig. 1D) and we thus looked for photographs taken between September 2003 and May 2005. This was carried out by looking at the Exif metadata which are publicly available within the three above-mentioned imagery repositories. After a visual checking, 30 pictures taken from different viewpoints and with a mean size of 500 Ko were selected (Fig. 2 and Appendix A). Note that due to a limited number of available images, we were forced to choose pictures taken in different seasons. However, snow is hardly present in the steep Drus faces and its influence can be neglected on the winter images.

<< FIGURE 2 >>

2.2 Ground-based LiDAR data acquisition

In order to scan the entire Drus West face with a high density of points (~250 points/m^2), we conducted seven LiDAR measurement campaigns from October 2005 to November 2011. The 2005 to 2010 point clouds represent only the upper part of the face and were acquired from the Flammes de Pierre ridge (Fig. 2) with a medium-range laser scanner (Optech ILRIS-3D) (Ravanel and Deline, 2006). The 2011 scans of the whole face have been taken with a long-range laser scanner (Optech ILRIS-LR) from the right lateral moraine of the Glacier des Drus, around 2'500 m a.s.l. (Fig. 2), delivering a higher number

Nat. Hazards Earth Syst. Sci. Discuss., doi:10.5194/nhess-2016-316, 2016
Manuscript under review for journal Nat. Hazards Earth Syst. Sci.
Published: 7 October 2016

Natural Hazards and Earth System Sciences Discussions

of points (9 and 25 million points respectively). These datasets were then processed with Iterative Closest Point (ICP) algorithms (Besl and McKay, 1992) in order to align and georeference the point clouds. The georeferencing was performed using accurate GPS measurements. However, between these two acquisitions, two major rockfalls occurred in September 2011 (4'530 ± 200 m^3) and October 2011 (54'730 ± 400 m^3) in the main rock-avalanche scar area (Fig. 4). These volumes were determined by comparing the 2005 and 2011 terrestrial LiDAR acquisitions. Thus, a volume of 59'260 m^3 is to be subtract from the estimated volume for the pillar collapse, given by the result of the comparison between the pre (SfM model) and post-event (2011 LiDAR scans).

2.3 Construction of the SfM point cloud

The workflow of Agisoft PhotoScan was used to construct a dense point cloud of the former Drus West face. All selected pictures were aligned during this procedure and the final model (Fig. 2) that represents the north-western side of the Aiguille Verte and Drus consists of 895'300 points, with a mean density of 0.5 points/m^2. The SfM point cloud was then scaled and georeferenced on the LiDAR point clouds by selecting several equivalent point pairs (a dozen) sufficiently distant from each other. Note that this procedure was carried out with 3DReshaper and no ground control points have been imposed when generating the 3D model on Agisoft PhotoScan. Finally, ICP algorithms (Besl and McKay, 1992) have been used to precisely align both point clouds.

2.4 SfM/LiDAR comparison and rockfall extraction

The first step to perform a point-to-mesh comparison was to transform the georeferenced LiDAR point clouds into a triangular mesh. All the points were used for the reference mesh creation and a maximum length of triangle edge of 5 m was set to fill the existing holes in the point clouds (zones masked by the relief). Unlike the point-to-point comparison, the point-to-mesh comparison calculates the orthogonal distance between both entities, which corresponds to the shortest distance between a point and the nearest triangle. Figure 3 shows the result of this comparison but also the points (in red on the right picture) that were extracted from the SfM cloud and associated with the Bonatti Pillar collapse. The point extraction was carried out by following the method defined by Tonini and Abellán (2014). This includes three steps: (a) definition of a level of detection (± 3 m in our case), (b) Feature extraction using the Nearest Neighbor Clutter Removal algorithm (Byers and Raftery, 1998) and (c) Single rockfall recognition with the DBSCAN algorithm (Ester et al., 1996) which is based on the spatial density of points.

<< FIGURE 3 >>

2.5 Volume calculation

We estimated the 2005 rock-avalanche volume by constructing a watertight mesh. For this purpose, the points extracted from the SfM cloud were first converted into a triangular mesh to create a closed surface whose contour (the free border) has been

Nat. Hazards Earth Syst. Sci. Discuss., doi:10.5194/nhess-2016-316, 2016
Manuscript under review for journal Nat. Hazards Earth Syst. Sci.
Published: 7 October 2016

Natural Hazards and Earth System Sciences Discussions

extracted automatically. This contour (3D polyline) was then orthogonally projected onto the reference mesh in order to divide it into two parts and keep only the triangles located inside the projected contour (delimitation of the rockfall scar). The gap between both contours was filled by a third mesh, which corresponds to the thickness of the fallen volume. Finally, we merged the three surfaces to generate a closed mesh. The volume of the rockfall event is then given by the sum of the tetrahedrons volumes forming the watertight mesh. In addition, in order to assess an error on the volume calculation, we created two other SfM models by importing respectively 84 and 67 % of the pictures used to construct the first point cloud.

3 Results and discussion

The comparison between the SfM point cloud and the LiDAR mesh of November 2011 gives a volume of 351'940 m^3 (Fig. 4A and 4B). This volume includes the rockfall events that occurred in September and October 2011 and we had to subtract 59'260 m^3 (Fig. 4D) from this value to properly assess the 2005 rock-avalanche volume. Therefore, the final value is equal to 292'680 m^3, which is quite close to the 265'000 ± 10'000 m^3 estimated by Ravanel and Deline (2008). Furthermore, the volumes estimated with the two other SfM models are respectively equal to 311'970 and 326'240 m^3. Thus, if we consider an average volume of 311'970 m^3, the relative error ranges between 4 and 6 %. Given the large difference of density of points observed between the SfM model and the LiDAR point clouds (500 times higher for the LiDAR), this uncertainty value is acceptable and consistent (same order of magnitude) with the one given by Ravanel and Deline (2008). The low density of points (0.5 points/m^2) of the SfM cloud is also found in the overall shape of the calculated volume, which is quite rounded (Fig. 4A) and lacks morphological details such as overhangs visible in the upper part of the Bonatti Pillar (Fig. 1D). This lack of details is due to the medium resolution of the images that we used to generate the SfM model, and also to the fact that most of the photographs were taken far from the face (Fig. 2). In contrast, we could reproduce accurately the lateral boundaries of the collapsed volume as well as the height of the Bonatti Pillar. Figure 4C perfectly illustrates this aspect since the 2005 rock-avalanche volume exceeds only in one place (at the top left) the scar limits (white dashed line) defined by Fort et al. (2009). Besides, this difference is normal because this area corresponds to the upper part of the October 2011 rockfall event (Fig. 4D).

<< FIGURE 4 >>

The rounded shape of the volume determined from the coupling SfM/LiDAR suggests that the 292'680 m^3 (± 5 %) calculated could be overestimated. The result shown in Fig. 3 heads in this direction since the positive deviations observed inside the ellipses do not correspond to rockfall events (verified on pictures), but artefacts that form "tips" in the SfM point cloud. These "tips" are also visible in the right part of Fig. 3 (see the white ellipse and the longitudinal profile that passes through the LiDAR and SfM point clouds) and probably present within the red points assigned to the Bonatti Pillar collapse, which could logically increase the volume calculation. These local deformations are certainly linked to the fact that the

Nat. Hazards Earth Syst. Sci. Discuss., doi:10.5194/nhess-2016-316, 2016
Manuscript under review for journal Nat. Hazards Earth Syst. Sci.
Published: 7 October 2016

Natural Hazards and Earth System Sciences Discussions

selected images were taken in different seasons and with different lighting-shading conditions (Fig. 2). In addition, the fact that we didn't impose ground control points during the SfM point cloud generation adds uncertainty to the model. However in this work, we were not looking for a highly accurate volume but to assess the potential of merging terrestrial LiDAR acquisitions with SfM made from web-retrieved images for quantifying past natural disasters. With this in mind, it was possible to define a range of relative error for the volume calculation according to the number of pictures used to generate the SFM model: 9 % in the case of 30 pictures (overestimation of 27'680 m^3 compared to the value of 265'000 m^3) and 19 % with 20 pictures (overestimation of 61'240 m^3). This suggests that the accuracy of the volume could be improved if more than 30 images would have been available. Note that these error percentages could have been higher if the level of detection chosen (± 3 m due to the high level of measurement noise characterizing the SfM model, see Fig. 3) was lower (e.g. ± 2 m) since more points would have been extracted from the comparison and associated with the volume of the June 2005 rock-avalanche. Nevertheless, it is not excluded that the volume determined by Ravanel and Deline in 2008 is slightly underestimated because even if accurate measurements were performed on the LiDAR mesh of October 2005, there is no 3D model available before the collapse. For such volume ranges, it is often the depth that is difficult to correctly assess and a small variation (e.g. 50 cm) can modify the final result of several thousands of m^3. In the specific case of the Bonatti Pillar (500 m high for 80 m wide), a depth variation of 50 cm could change the final volume of about 20'000 m^3. Finally, it is important to specify that both volumes fallen in September and October 2011 play a significant role in our estimations. However, given the uncertainties mentioned in section 2.2 – the volumes were calculated by comparing the 2005 LiDAR point clouds of the Flammes de Pierre to the 2011 LiDAR triangular mesh of the Glacier des Drus – the values are pretty accurate and it is not these estimations that most influence the final result.

4 Conclusion

The method described in this Short Note has worked remarkably well for the Petit Dru West face, which is a legendary peak photographed since decades and from several corners of the Chamonix Mont-Blanc Valley. However, it is important to highlight that the same method would have been difficult to implement on a less well-known site, where fewer images could have been collected and downloaded from picture hosting services on the World Wide Web. Another issue may be the limited number of viewpoints that exist on a study site because it is necessary to turn around the area of interest to create a good quality SfM model. In the field of natural hazards, digitizing of old photographs coupled to SfM methods is to be taken into account because it can deliver extremely useful data on the morphologies of the past. In some cases, this could allow to go back to the beginning of the last century and even in 1860 for the Drus with the different photographs (daguerreotypes) of the Bisson brothers.

Acknowledgements

The authors would like to acknowledge the Swiss National Science Foundation (SNSF, grants 200020_146426 and 200020_159221) for supporting this research. Second author was granted with a Marie Curie fellowship (Project ref.: 705215). In addition, we would like to thank the authors of the pictures extracted from *Flickr*, *SummitPost* and *CamptoCamp* (see Appendix A for a detailed description). Finally, the support of the Chamonix Mont-Blanc Helicopters (CMBH) company for reaching the stations from which terrestrial LiDAR acquisitions were performed is also acknowledged.

Appendix A: Photo credits

Links to the 30 web-retrieved images that were downloaded from the following websites: *Flickr.com*, *SummitPost.org* and *Camptocamp.org*.

Flickr.com (15)

https://www.flickr.com/photos/42624864@N08/5765604229
https://www.flickr.com/photos/markhorrell/17225632811
https://www.flickr.com/photos/phileole/520418709
https://www.flickr.com/photos/phileole/520390144
https://www.flickr.com/photos/phileole/520419341
https://www.flickr.com/photos/mvcchris/9697023856
https://www.flickr.com/photos/robonabike/4568776704
https://www.flickr.com/photos/francoisdorothe/5451738425
https://www.flickr.com/photos/29922628@N08/3192264930
https://www.flickr.com/photos/davduf/1075398
https://www.flickr.com/photos/bengalshare/952842570
https://www.flickr.com/photos/tsa-climbing/6505792537
https://www.flickr.com/photos/ebbandflow/4500495087
https://www.flickr.com/photos/ebbandflow/4501086770
https://www.flickr.com/photos/jd-davis/15930404616

SummitPost.org (12)

http://www.summitpost.org/the-dru-as-seen-from-the-gran/40929/c-150757
http://www.summitpost.org/aiguille-verte/84226/c-183839
http://www.summitpost.org/aiguille-verte/84227/c-183839
http://www.summitpost.org/at-sunset-in-winter/85906/c-150757

http://www.summitpost.org/les-drus-from-mere-de-glace/116269/c-150757
http://www.summitpost.org/aiguille-du-dru/112906/c-182555
http://www.summitpost.org/aiguille-du-dru/112230/c-182555
http://www.summitpost.org/aiguille-verte/112911/c-182555
http://www.summitpost.org/aiguille-du-dru-flammes-de-pierre/112907/c-182555
http://www.summitpost.org/petit-dru/108236/c-150757
http://www.summitpost.org/petit-dru/108291/c-150757
http://www.summitpost.org/les-drus-by-sjaak-de-visser/108214/c-150757

Camptocamp.org (3)
http://s.camptocamp.org/uploads/images/1059260673_1126855737.jpg
http://s.camptocamp.org/uploads/images/1002626915_1423457826.jpg
http://s.camptocamp.org/uploads/images/1286183275_392583017.jpg

References

Abellán, A., Derron, M. H., & Jaboyedoff, M. (2016): "Use of 3D Point Clouds in Geohazards" Special Issue: Current Challenges and Future Trends. Remote Sensing, 8(2), 130.

AgiSoft, L. L. C. (2014): Agisoft PhotoScan Professional Edition (version 1.0. 3).

Besl, P. J., & McKay, N. D. (1992): Method for registration of 3-D shapes. In Robotics-DL tentative (pp. 586-606). International Society for Optics and Photonics.

Bussy, F., Schaltegger, U., & Marro, C. (1989): The age of the Mont-Blanc granite (Western Alps): a heterogeneous isotopic systeme dated by Rb-Sr whole rock determinations on its microgranular enclaves. Schweizerische Mineralogische und Petrographische Mitteilungen, 69(1), 3-13.

Byers, S., & Raftery, A. E. (1998): Nearest-neighbor clutter removal for estimating features in spatial point processes. Journal of the American Statistical Association, 93(442), 577-584.

Doulamis, A., Ioannides, M., Doulamis, N., Hadjiprocopis, A., Fritsch, D., Balet, O., ... & Johnsons, P. S. (2013): 4D reconstruction of the past. In First International Conference on Remote Sensing and Geoinformation of Environment (pp. 87950J-87950J). International Society for Optics and Photonics.

Egli, D., & Mancktelow, N. (2013): The structural history of the Mont Blanc massif with regard to models for its recent exhumation. Swiss Journal of Geosciences, 106(3), 469-489.

Ester, M., Kriegel, H. P., Sander, J., & Xu, X. (1996): A density-based algorithm for discovering clusters in large spatial databases with noise. In Kdd (Vol. 96, No. 34, pp. 226-231).

Estrin, J. (2012): "In an Age of Likes, Commonplace Images Prevail". The New York Times' Lens Blog, 7 Sep. 2012.

Firpo, G., Salvini, R., Francioni, M., & Ranjith, P. G. (2011): Use of digital terrestrial photogrammetry in rocky slope stability analysis by distinct elements numerical methods. International Journal of Rock Mechanics and Mining Sciences, 48(7), 1045-1054.

Fonstad, M. A., Dietrich, J. T., Courville, B. C., Jensen, J. L., & Carbonneau, P. E. (2013): Topographic structure from motion: a new development in photogrammetric measurement. Earth Surface Processes and Landforms, 38(4), 421-430.

Fort, M., Cossart, E., Deline, P., Dzikowski, M., Nicoud, G., Ravanel, L., ... & Wassmer, P. (2009): Geomorphic impacts of large and rapid mass movements: a review (Vol. 15, No. 1, pp. 47-64). Groupe français de géomorphologie.

Furukawa, Y., Curless, B., Seitz, S. M., & Szeliski, R. (2010): Towards internet-scale multi-view stereo. In Computer Vision and Pattern Recognition (CVPR), 2010 IEEE Conference on (pp. 1434-1441). IEEE.

Grün, A., Remondino, F., & Zhang, L. (2004): Photogrammetric reconstruction of the great Buddha of Bamiyan, Afghanistan. The Photogrammetric Record, 19(107), 177-199.

Grün, A., Remondino, F., & Zhang, L. (2005): The Bamiyan project: multi-resolution image-based modeling. Recording, Modeling and Visualization of Cultural Heritage, 415(39208), 45-54.

Ioannides, M., Hadjiprocopi, A., Doulamis, N., Doulamis, A., Protopapadakis, E., Makantasis, K., ... & Julien, M. (2013): Online 4D reconstruction using multi-images available under Open Access. ISPRS Ann Photogramm Remote Sens Spat Inf Sci, 5, W1.

James, M. R., & Robson, S. (2014): Mitigating systematic error in topographic models derived from UAV and ground-based image networks. Earth Surface Processes and Landforms, 39(10), 1413-1420.

Kyriakaki, G., Doulamis, A., Doulamis, N., Ioannides, M., Makantasis, K., Protopapadakis, E., ... & Weinlinger, G. (2014): 4D Reconstruction of Tangible Cultural Heritage Objects from Web-Retrieved Images. International Journal of Heritage in the Digital Era, 3(2), 431-451.

Leloup, P. H., Arnaud, N., Sobel, E. R., & Lacassin, R. (2005): Alpine thermal and structural evolution of the highest external crystalline massif: The Mont Blanc. Tectonics, 24(4).

Lucieer, A., de Jong, S., & Turner, D. (2014): Mapping landslide displacements using Structure from Motion (SfM) and image correlation of multi-temporal UAV photography. Progress in Physical Geography, 0309133313515293.

Matasci, B., Jaboyedoff, M., Ravanel, L., & Deline, P. (2015): Stability Assessment, Potential Collapses and Future Evolution of the West Face of the Drus (3,754 m asl, Mont Blanc Massif). In Engineering Geology for Society and Territory-Volume 2 (pp. 791-795). Springer International Publishing.

Oikonomidis, D., Albanakis, K., Pavlides, S., & Fytikas, M. (2016): Reconstruction of the paleo-coastline of Santorini island (Greece), after the 1613 BC volcanic eruption: A GIS-based quantitative methodology. Journal of Earth System Science, 125(1), 1-11.

von Raumer, J. F., & Bussy, F. (2004): Mont Blanc and Aiguilles Rouges: Geology of Their Polymetamorphic Basement (external Massifs, Western Alps, France-Switzerland). Université de Lausanne-Section des sciences de la terre.

Ravanel, L., & Deline, P. (2006): Nouvelles méthodes d'étude de l'évolution des parois rocheuses de haute montagne: application au cas des Drus. In Proceedings of the workshop «Géologie et Risques Naturels: la gestion des risques au Pays du Mont Blanc» (pp. 48-53).

Ravanel, L., & Deline, P. (2008): La face ouest des Drus (massif du Mont-Blanc): évolution de l'instabilité d'une paroi rocheuse dans la haute montagne alpine depuis la fin du petit âge glaciaire. Géomorphologie: relief, processus, environnement, 14(4), 261-272.

Santos, P., Serna, S. P., Stork, A., & Fellner, D. (2014): The Potential of 3D internet in the cultural heritage domain. In 3D Research Challenges in Cultural Heritage (pp. 1-17). Springer Berlin Heidelberg.

Salvini, R., Francioni, M., Riccucci, S., Bonciani, F., & Callegari, I. (2013): Photogrammetry and laser scanning for analyzing slope stability and rock fall runout along the Domodossola–Iselle railway, the Italian Alps. Geomorphology, 185, 110-122.

Snavely, N., Seitz, S. M., & Szeliski, R. (2008): Modeling the world from internet photo collections. International Journal of Computer Vision, 80(2), 189-210.

Stathopoulou, E. K., Georgopoulos, A., Panagiotopoulos, G., & Kaliampakos, D. (2015): Crowdsourcing Lost Cultural Heritage. ISPRS Annals of the Photogrammetry, Remote Sensing and Spatial Information Sciences, 2(5), 295.

Technodigit (2014): 3DReshaper: the 3D Scanner Software (Version 2014 MR1) [Computer software]. http://www.3dreshaper.com/.

Tonini, M., & Abellán, A. (2014): Rockfall detection from terrestrial LiDAR point clouds: A clustering approach using R. Journal of Spatial Information Science, 2014(8), 95-110.

Turner, D., Lucieer, A., & Watson, C. (2012): An automated technique for generating georectified mosaics from ultra-high resolution unmanned aerial vehicle (UAV) imagery, based on structure from motion (SfM) point clouds. Remote Sensing, 4(5), 1392-1410.

Vincent, M. L., Gutierrez, M. F., Coughenour, C., Manuel, V., Bendicho, L. M., Remondino, F., & Fritsch, D. (2015): Crowd-sourcing the 3D digital reconstructions of lost cultural heritage. In 2015 Digital Heritage (Vol. 1, pp. 171-172). IEEE.

Nat. Hazards Earth Syst. Sci. Discuss., doi:10.5194/nhess-2016-316, 2016
Manuscript under review for journal Nat. Hazards Earth Syst. Sci.
Published: 7 October 2016

Natural Hazards and Earth System Sciences
Discussions

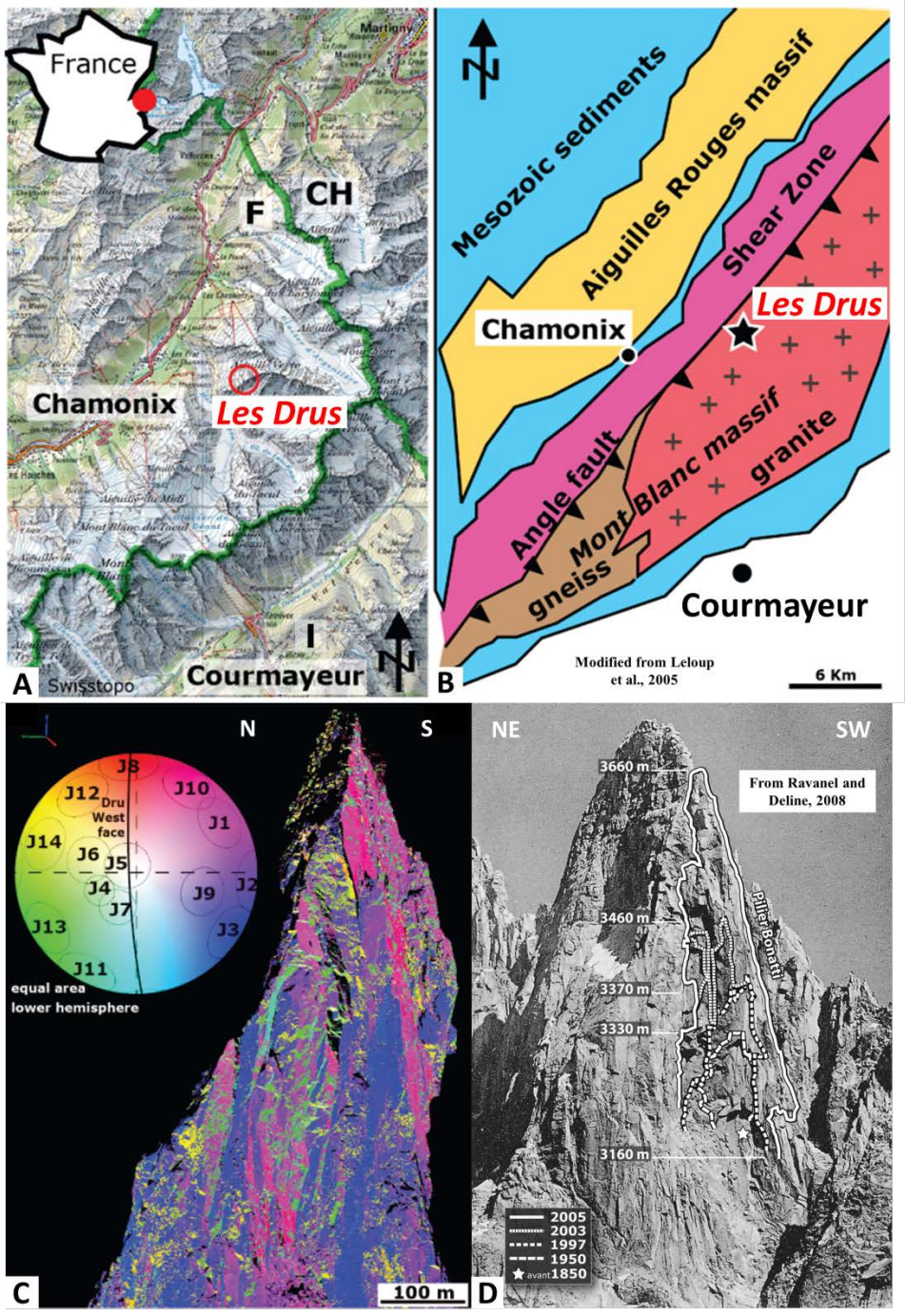

Figure 1: Location and geological setting of the study area. A: Location of the Drus Mountain within the Chamonix Valley (Mont-Blanc massif, France); background map: Swisstopo. B: Geological map of the study area (after Leloup et al., 2005). C: 2011 LiDAR point cloud and discontinuities measured in the Drus West face. Each color corresponds to the stereographic projection of the poles of joint sets (Schmidt stereoplot, Coltop3D software). D: Photo-comparison reconstruction of the main historical rockfall events occurred in the Drus West face since 1850 (figure modified after Ravanel and Deline, 2008).

Nat. Hazards Earth Syst. Sci. Discuss., doi:10.5194/nhess-2016-316, 2016
Manuscript under review for journal Nat. Hazards Earth Syst. Sci.
Published: 7 October 2016

Natural Hazards and Earth System Sciences
Discussions
Open Access
EGU

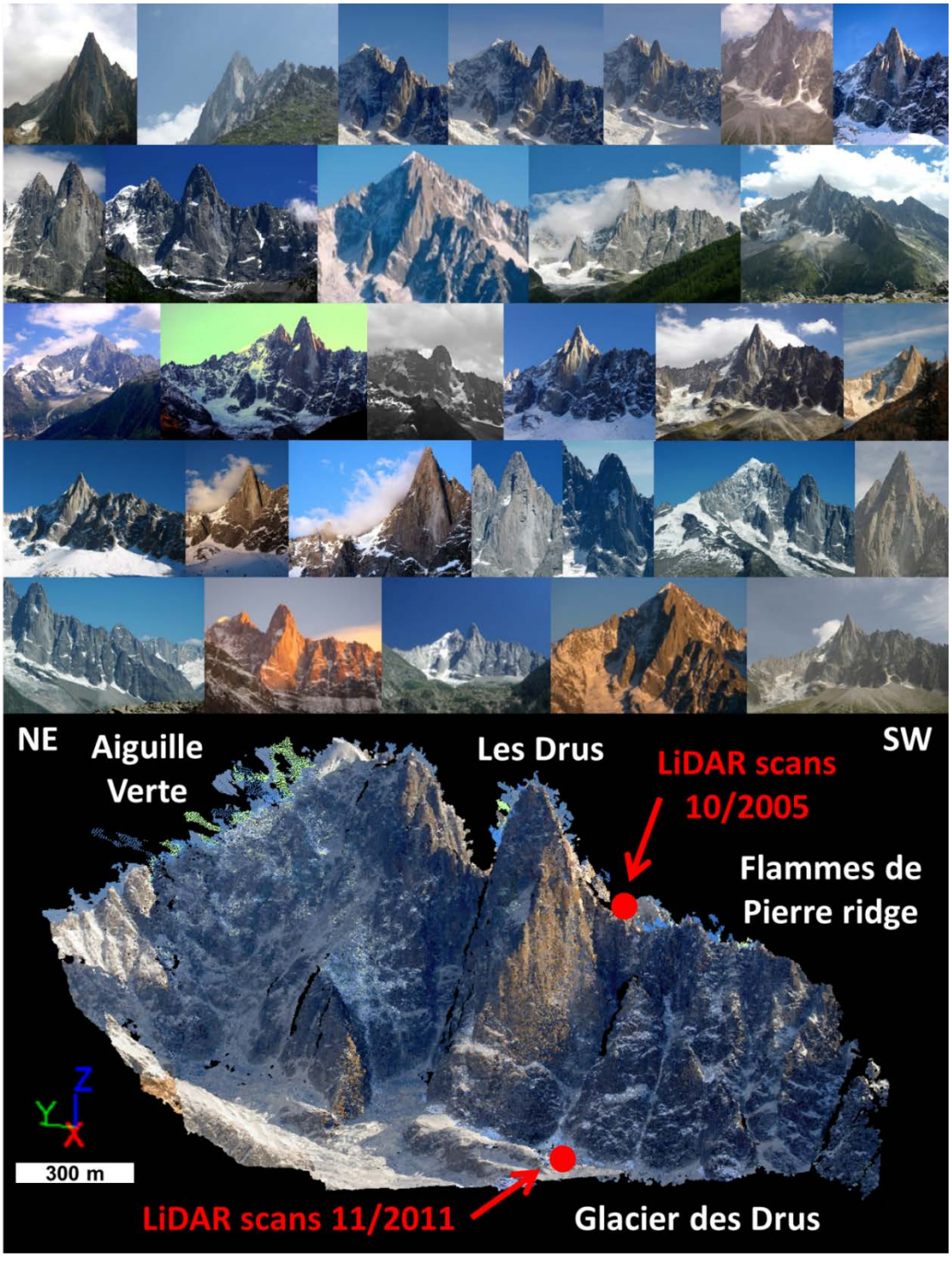

Figure 2: Catalogue of the 30 pictures selected on the Internet (upper part, links available in the Appendix A) and used to reconstruct the north-western side of the Aiguille Verte and Drus (lower part, SfM point cloud) before the Bonatti Pillar collapse in June 2005. Both red dots show the location of the 2005 and 2011 ground-based LiDAR acquisitions.

Nat. Hazards Earth Syst. Sci. Discuss., doi:10.5194/nhess-2016-316, 2016
Manuscript under review for journal Nat. Hazards Earth Syst. Sci.
Published: 7 October 2016

Natural Hazards and Earth System Sciences
Discussions

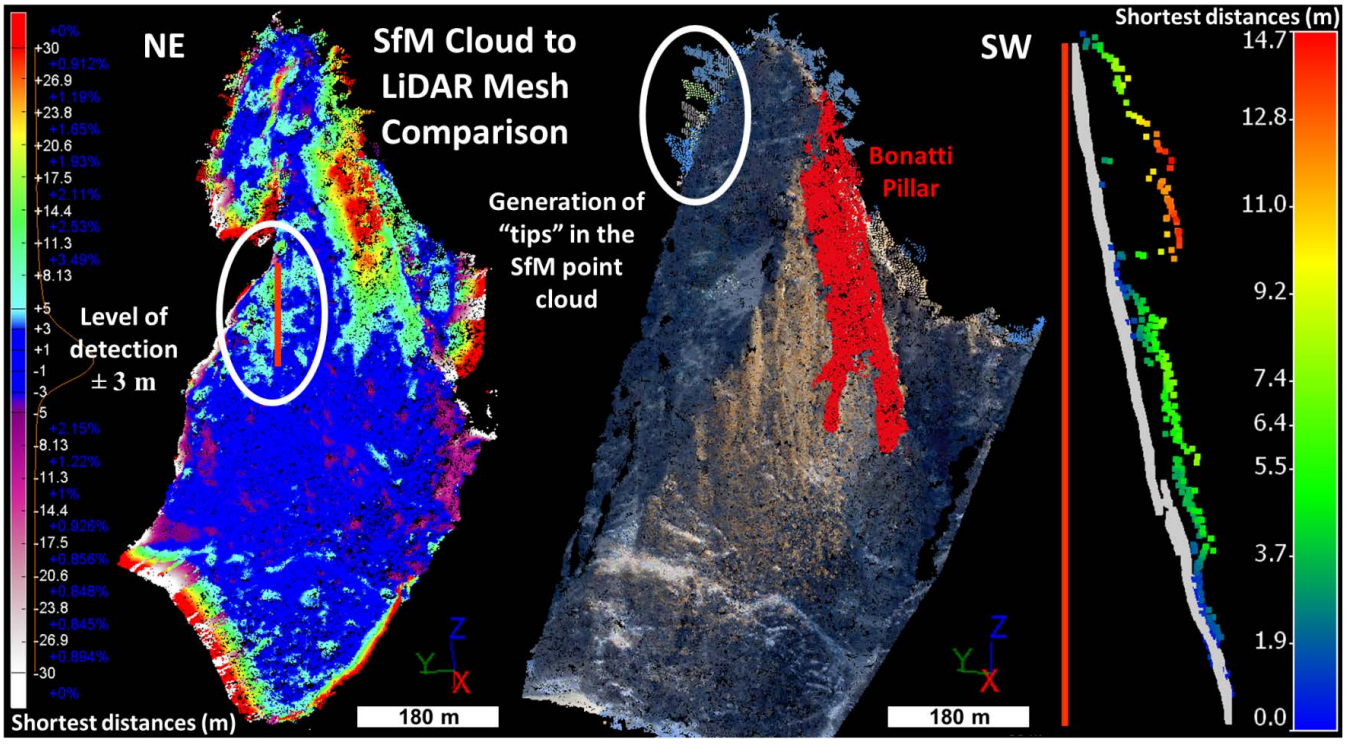

Figure 3: Result of the point-to-mesh comparison (left) between the SfM point cloud and the reference LiDAR mesh of November 2011. The color scale of the shortest distances is divided in two parts: positive deviations from blue to red and negative deviations from blue to white. The points extracted from this comparison and associated with the 2005 rock-avalanche were then highlighted in red on the SfM model of the Drus Mountain (right image). The two white ellipses illustrate the artefacts that form "tips" in the SfM model and the red line located in the center of the left ellipse corresponds to a longitudinal cross-section that passes through the LiDAR and SfM point clouds. This cross-section is visible in the right side of the figure; grey points correspond to the LiDAR dataset, while colored points come from the SfM dataset.

Nat. Hazards Earth Syst. Sci. Discuss., doi:10.5194/nhess-2016-316, 2016
Manuscript under review for journal Nat. Hazards Earth Syst. Sci.
Published: 7 October 2016

Natural Hazards and Earth System Sciences
Discussions

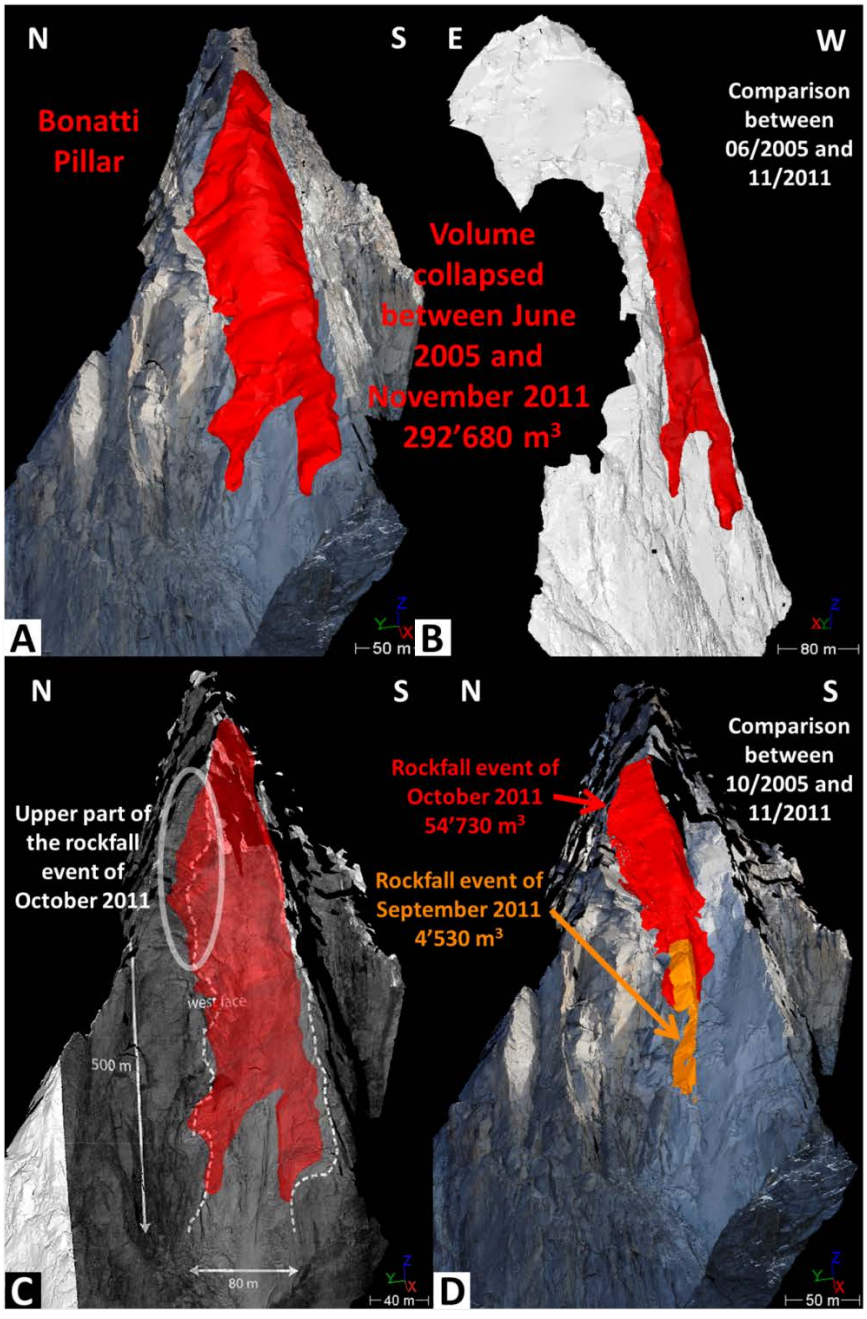

Figure 4: 3D geometry of the volumes collapsed between June 2005 and November 2011. A: Photorealistic model of the Drus West face (high-resolution LiDAR mesh textured with a picture of November 2011) and front view of the volume (in red) calculated with 3DReshaper. B: Side view of the high-resolution LiDAR mesh (non-textured) as well as the volume shown in Fig. 4A. C: Superimposition of the volume collapsed between June 2005 and November 2011 with another photorealistic model, textured from the left part of the Fig. 8 of Fort et al. (2009). The white dashed line shows the scar limits of the June 2005 rock-avalanche and the white ellipse illustrates the area that corresponds to the upper part of the October 2011 rockfall event. D: Photorealistic model of the Drus West face and front view of the rockfall events occurred in September (in orange) and October 2011 (in red).